Spectroscopic Characterization, Homo-Lumo, NBO study by DFT and Molecular Docking Studies of 2-Amino-6-Metheylpyridine

Mahalakshmi G[1], Subha V[2], Sheena Mary Y[3] & Balachandran V[4]
[1,2,]Research Department of Physics, Government Arts College(Autonomous), Karur - 639 005, India.
[3]Department of Physics, Fatima Mata National College, Kollam, Kerala, India
[4]Research Department of Physics, Arignar Anna Government Arts College, Musiri, Tiruchirapalli 621211, India.

Received: June 12, 2018 Accepted: July 29, 2018

ABSTRACT *The FT-IR (4000-400 cm-1) and FT-Raman (3500 - 0 cm-1) spectra have been recorded on the strong period of the 2-amino-6-methyl pyridine (2A6MP) molecule. The DFT strategy (Density Functional Theory) helps in perceiving the holding highlights and harmonica vibrational frequencies and the equilibrium geometry. "Everything has been performed with reference to vitality appropriation (TED) of the vibrational modes, computed with scaled quantum mechanical power field procedure (SQMFF)". The molecule geometry, holding highlights, energy gap and Natural Bond Orbital (NBO) examination of 2A6MP in ground state were gotten by DFT with standard B3LYP/6-311+G(d, p) premise set mixes. Besides, the NBO examination on comparative structures like substitution of H9, H10, H11 by Cl9, Cl10, Cl11 (2-3-, 4C2A6MP) in the title particle improved the situation various intra-molecular collaborations that are intended for the atom adjustment. The energy gap, polarizabilities and first hyper polarizabilities calculations were also done on 2-3-,4-C2A6MP. The studies of Molecular docking were done with apt protein (Source: Protein Data Bank)*

Keywords: *2-amino-6-methyl pyridine(2A6MP), FT-IR,FT-Raman, DFT studies, NBO, HOMO-LUMO, Molecular Docking.*

Introduction

The vibrational spectrum and structure spectrum of pyridine`s derivatives are important because of the involvement in bioactivities and applications in pharma, agricultural & other domains [1-3]. The medicinal value of heterocyclic compounds helps in the attraction of 2-amino pyridine derivatives [4, 5]. Pyridine is mixed with ethanol to make it not suitable for drinking. For synthesizing DNA[6], sulfapyridine (a drug against various infections of Bacteria and virus), antihistaminic drugs tripelennamine & mepyramine, water repellents, herbicides and killing bacteria. The Ring formation is found in some chemical compounds even though it's not from pyridine synthesis. It includes Vitamin B niacin & pyridoxine, isoniazid antituberculosis drug, nicotine and plants which contains nitrogen[7]. From Coal Tar Pyridine is produced which is the buy product of gasification of the coal. The spike in requirement of Pyridine resulted in synthesizing from acetaldehyde and ammonia in more affordable methods which yields 20,000 tons per year.

A hetero aromatic compound which is miscible with water & organic solvents [8]. Crystalline hydrochloride salt is formed when its mixed with HCl which melts at 145-147 °C [9]. During organic reactions, pyridine behaves both as a "tertiary amine (protonation, alkylation, acylation, and N-oxidation at the nitrogen atom) and also as aromatic compound"(undergoing nucleophilic substitutions). It is electron deficient due to the presence of electronegative nitrogen in the pyridine ring. So it undergoes soon an electrophilic aromatic replacement reactions which depicts a benzene derivatives; the unbound reactions will not look for protons (prorogated pyridine is always electron-deficient). Pyridine inclines to nucleophilic substitution metalation of the ring by strong organ metallic bases not like Benzene [10-11]. Three chemical clusters are noted for the reactivity of pyridine. Pyridine enunciates aromatic properties during electrophilic substitution with electrophiles. The capability of pyridine and its derivatives to oxidize, which helps in forming the amine oxides (*N*-oxides), which is of the nature of tertiary amines [12]. Lone pair of electrons because of pyridine`s nitrogen center which is not part of aromatic ring, having the chemical properties of tertiary amines. By donating its pair of electrons to a Lewis acid as in the sulfur trioxide pyridine complex it can perform as a Lewis base. The complexes forming with transition of metals ions make pyridine a weak ligand [13].

The geometry of isomeric pyridines was examined by X-ray crystallography [14], microwave spectroscopy [15] and surface-enhanced Raman spectroscopy [16]. DFT vibrational studies of 5-bromo-2-nitropyridine [17], pyridinium complexes [18], and 2-chloro-5-bromopyridine [19] were stated. Tautomerization and rotamerization of amino pyridines has been described [20]. The vibration (IR and Raman) spectra of amino pyridines, methyl-substituted amino pyridines and hydrogen chlorides of amino

pyridines had been identified by spinner experimentally [21]. However, to the best of our knowledge, according to literature survey there is no results based on quantum chemical calculations, FT-IR/FT-Raman spectral studies on (2A6MP). We have documented comprehensive interpretations of the infrared and Raman spectra based on the experimental and theoretical results.

Experimental and computational details

The title compounds were obtained from Sigma –Aldrich Chemical Company (USA), with a stated purity of greater than 98% and it was used as such without further purification. The FT-Raman range of 2A6MP atom has been recorded utilizing the 1064 nm line of a Nd:YAG laser as excitation wavelength in the district 400 – 4000 cm^{-1} on a BRUCKER demonstrate IFS 66V spectrometer. The detailed wave numbers are relied upon to the precise inside 1 or -1 cm^{-1}. The FT-IR range of this compound was recorded in the district 0 – 3500 cm^{-1}on IFS 66V spectrometer furnished with a MCT identifier utilizing KBr bar splitter and Globar source. The information were recorded in the co-expansion of 200 scans at 1 or -1cm resolution with 250mW of intensity at the example in both the methods.

Computations was performed at B3LYP/6-311+G(d, p) substantial premise set on PC utilizing Gaussian 09W[22] program bundle, summoning slope geometry streamlining, wave numbers, polarizability esteems, outskirts sub-atomic orbital investigation, NBO[23]. Moreover the unscaled computed wave numbers, drive constants, infrared forces and Raman exercises are received. The vibrational investigation got for 2A6MP with the unscaled B3LYP/6-311+G (d, p) force field are more prominent than the trial esteems because of disregard of anharmonicity in genuine frame work. It ought to be noticed that the test results belongs to solid stage and theoretical calculations belong to gaseous stage. These disparities can be revised either by figuring anharmonic remedies unequivocally or by presenting a scaled field or straightforwardly scaling the examined wave numbers with legitimate factor [24]. A provisional task is frequently made based on the unscaled frequencies by expecting the watched frequencies with the goal that they are same manner as examined one. At that point, for a less demanding correlation with the examined value, the calculated frequencies are scaled by the scale to less than 1, to minimize the general deviations. A superior assertion between the calculated and tested frequencies can be gotten by utilizing distinctive scale factors for various regions of vibrations. For that reason, we have used diverse scaling factors for every single essential mode aside from the torsional mode to get the scaled frequencies of the compound.

Result and discussion

Geometrical parameters

Before computing the frequencies and electronic properties, it is necessary to analyze the molecular structure of the compound. So that the structure is optimized at DFT/B3LYP/6-311+G(d, p) level of theory and numbering scheme is represented in **Fig. 1** and the calculated optimized geometrical parameters are presented in **Table 1**. To the best of our knowledge, no X-ray crystallography data of the 2A6MP molecule has yet been established. Be that as it may, the ascertained outcomes acquired are relatively synonymous with the announced structural parameters of similar molecules. For 2-Amino-6-methylpyridinium 2-carboxybenzoate [25], C-N bond lengths C2-N1=1.350Å , C6-N1=1.369 Å and C2-N8=1.326 Å . For 2-Amino-6-methylpridinium 4-methyl-benzenesulfonate [26], C-N bond lengths C6-N1=1.358Å , C2-N1=1.338 Å and C2-N8=1.368 Å. The C-N bond length in pyridine ring of the title compound C6-N1=1.358 Å , C2-N1 =1.358 Å and C2-N8=1.462 Å is significantly shorter than the typical C-N single bond that is alluded to 1.49 Å , which affirms this attach to have some character of a doubled or conjugated bond[27]. For this situation, H9 and H10 to ring C2 and C3 separate is 1.1 Å moderately 0.17 Å longer than the x-ray diffraction [25] because of the electron pulling back impacts relying upon the nearness of the – NH2, - CH3 clusters connected to these bonds. The DFT calculation predict the bond angles within the pyridine ring, C3-C2-N1=122.6°, C2-C3-C4=117.9°, C3-C4-C5= 119.8°, C4-C5-C6=118.4°, C5-C6-N1=122.2° and C2-N1-C6=119.1°, whereas the corresponding reported values are 118.1°, 119.1°, 121.3°, 119.6°, 118.4°, 123.6°[25] and 120.3°, 120.1°, 118.2°, 121.5°, 120.1°, 120.6°[26]. At N8 position, the bond angles are C2-N8-H15=114.6°, C2-N8-H16=117.7° and H15-N8-H16=115.2° and the asymmetry in angles is because of the cooperation between the pyridine ring and H9 atom. The CH3, NH2 and pyridine ring are planar from each other as is clear from the torsion angles, N1-C2-C3-C4=0.1°, C3-C2-N1-C5=-0.5°, C4-C5-C6-C7=-180.0° and C7-C6-N1-C2=-179.7°.

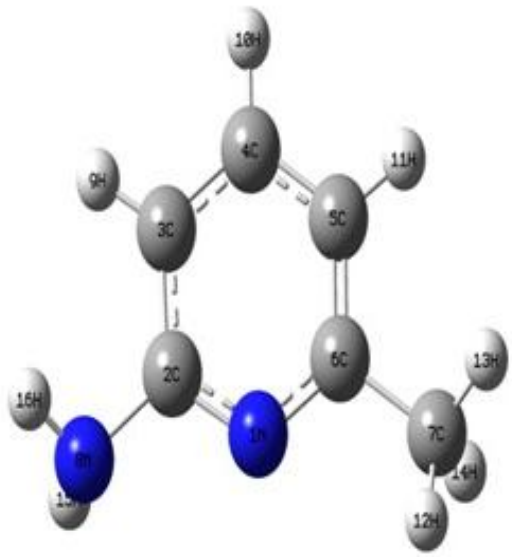

Fig. 1. The theoretical geometric structure and atoms numbering of 2A6MP

Table 1. Optimized geometrical parameters of 2-Amino-6-methylpyridine at B3LYP/6-311+G(d,p) level.

Bond length	Value (Å)	Expt.[a]	Expt.[b]	Bond Angle	Value (°)	Expt.[a]	Expt.[b]	Dihedral Angle	Value (°)
C2-C3	1.42	1.413	1.407	C3-C2-N1	122.6	118.1	120.3	N1-C2-C3-C4	0.1
C2-N1	1.358	1.350	1.338	C3-C2-N8	121.2	122.9	123	N1-C2-C3-H9	179.6
C2-N8	1.462	1.326	1.368	N1-C2-N8	116.2	119.0	116.7	N8-C2-C3-C4	-177.7
C3-C4	1.42	1.356	1.366	C2-C3-C4	117.9	119.1	120.1	N8-C2-C3-H9	1.9
C3-H9	1.1	0.93	1.896	C2-C3-H9	120.7	120.5	119.7	C3-C2-N1-C6	-0.5
C4-C5	1.42	1.397	1.390	C4-C3-H9	121.4	120.5	120.3	N8-C2-N1-C6	177.4
C4-H10	1.1	0.93	0.93	C3-C4-C5	119.8	121.3	118.2	C3-C2-N8-H15	-165.9
C5-C6	1.331	1.368	1.375	C3-C4-H10	120.0	119.4	120.9	C3-C2-N8-H16	-25.7
C5-C11	1.1	0.93	1.900	C5-C4-H10	120.3	119.4	120.9	N1-C2-N8-H15	16.2
C6-N1	1.358	1.369	1.358	C4-C5-C6	118.4	119.6	121.5	N1-C2-N8-H16	156.5
C6-C7	1.497	1.491	1.471	C4-C5-H11	121.0	120.2	117.8	C2-C3-C4-C5	0.3
C7-H12	1.113	0.96	0.96	C6-C5-H11	120.5	120.2	121.5	C2-C3-C4-H10	-179.9
C7-H13	1.113	0.96	0.96	C5-C6-N1	122.2	118.4	120.1	H9-C3-C4-C5	-179.2
C7-H14	1.113	0.96	0.96	C5-C6-C7	121.8	125.3	124.6	H9-C3-C4-H10	0.6
N8-H15	1.05	0.95	0.87	N1-C6-C7	116.0	116.4	115.3	C3-C4-C5-C6	-0.2
N8-H16	1.05	0.92	0.88	C2-N1-C6	119.1	123.6	120.6	C3-C4-C5-H11	179.8
				C6-C7-H12	110.2	109.5	109.5	H10-C4-C5-C6	180.0
				C6-C7-H13	111.7	109.5	109.5	H10-C4-C5-H11	0.0
				C6-C7-H14	110.2	109.5	109.5	C4-C5-C6-N1	-0.2
				H12-C7-H13	108.8	109.5	109.5	C4-C5-C6-C7	-180.0
				H12-C7-H14	107.1	109.5	109.5	H11-C5-C6-N1	179.7
				H13-C7-H14	108.7	109.5	109.5	H11-C5-C6-C7	0.0
				C2-N8-H15	114.6	122.3	123	C5-C6-N1-C2	0.5
				C2-N8-H16	117.7	119.1	117	C7-C6-N1-C2	-179.7
				H15-N8-H16	115.2	118	118	C5-C6-C7-H12	121.4
								C5-C6-C7-H13	0.4
								C5-C6-C7-H14	-120.6
								N1-C6-C7-H12	-58.3
								N1-C6-C7-H13	-179.4
								N1-C6-C7-H14	59.7

[a] X-ray data from Ref. [24][26].

[b] X-ray data from Ref. [24].

Vibrational assignments of the IR and Raman spectra

Understanding the point by point infrared and Raman natures of naturally active particles is basic for following purposes and also increasing progressed structural comprehension. Keeping in mind to additionally expand on the vibrational spectral properties of 2A6MP, the figured scaled wave numbers,

observed IR, Raman bands and point by point vibrational assignments for 2A6MP were given in Table 2. The watched (FT-IR and FT-Raman) spectra are appeared in **Fig. 2**.

NH_2 modes

The appearance of bands in 3600-3200 cm^{-1} region shows the presence of NH_2 group in the compound. The position, intensity and the breadth of the band indicate whether the group is free, exhibit intermolecular hydrogen bonding or is intra-molecularly bonded [28]. According to Socrates [29] the frequency of amino group appears around 3500–3300 cm^{-1} for NH_2 stretching, 1700 –1600 cm^{-1} for scissoring and 1150–900 cm^{-1} for rocking deformation. In the present study, the predicted strong band at 3536 cm^{-1} and 3331 cm^{-1} by DFT method was assigned to asymmetric and symmetric stretching mode of NH_2. The recorded band at 3324 cm^{-1} was assigned to asymmetric stretching mode of NH_2 and which are in agreement with the calculated values. Of course these two modes are extending modes as it is clear from TED, they are relatively contributing 99%. The NH_2 scissoring mode is allotted at 1609 cm^{-1} in FT-IR. The computed value of NH_2 scissoring is at 1610 cm^{-1}. The rocking mode is obtained at 994 cm^{-1} in Raman.

CH_3 modes

Saturated hydrocarbons contain methyl bunches demonstrated two different groups at 2962 cm^{-1} and at 2872 cm^{-1} [30]. The first of these outcomes from the not symmetrical extending mode as (ν_{as} CH_3) in which two C-H obligations of CH_3 aggregate are broadening while the third one in contracting. The second emerges from symmetrical extending (ν_{ss} CH_3) in which all the three CH bonds extended and contract in stage.

A noteworthy fortuitous event of theoretical qualities with that of trial assessments is found in the symmetric and asymmetric vibrations of the CH_3 moiety. The asymmetric extending for the NH_2, CH_2 extent higher than the symmetric extending [31]. The symmetric extending of CH_3 is seen in both FT-IR and FT-Raman is allocated at 2922 cm^{-1}. Parker [32] appointed these groups at 2930 and 2903 cm^{-1} in FT-IR and FT-Raman for N-methylmaleimide. The distortion method of CH_3 gatherings of title compound was typically exceedingly combined with other bending modes. The CH_3 bending is watched vibration band almost 1450 cm^{-1} [31, 33]. In this examination, the 1462 cm^{-1} FT-IR groups relate to inside bowing vibrations of the CH_3 cluster. DFT strategy concurs with the trial value. Parker [32] allocated CH_3 bending modes as 1440 and 1456 cm^{-1} both for FT-IR and FT-Raman. In methyl substituted molecule the symmetric disfigurement of CH_3 is required to show up in the range 1360-1390cm^{-1} [34] with a power fluctuating from frail to exceptionally solid. In this examination FT-IR and FT-Raman is assigned to 1379 and 1377 cm^{-1} individually. The processed wave numbers at 1361 cm^{-1} (B3LYP) is allocated to CH_3 symmetric bending for 2A6MP particle. Aromatic compounds show a methyl rock in the area of 1045 cm^{-1} [35]. It is valid from the above writing in our present investigation additionally the weak band saw in FT-IR range 1034 cm^{-1} is tagged to CH_3 rocking vibrations with TED commitment of 76%, the theoretically wave number for this mode is at 1038, 1136 cm^{-1}. As CH_3 torsional modes are normal underneath 100 cm^{-1}, the compound wave number at 47 cm^{-1} is tagged to CH_3 torsional mode.

CH modes

The most noticeable and informed bands in the spectra of aromatic compounds happen in the low frequency area between 675 - 900 cm^{-1}. The solid bonds initiates in the out-of-plane bending of the ring CH bonds [28]. The bands at 929, 785 and 736 in FT-IR and FT-Raman are related to CH out of plane bending methods of 2A6MP. The hetero aromatic structure demonstrates the occurrences of CH extending vibrations in the area 3100-3000 cm^{-1} which is identification are for the prepared distinguishing proof of CH extending vibrations [36, 37]. In the present work, the FT-Raman and FT-IR vibrational frequencies saw at 3066 and 3177cm^{-1} for 2A6MP have been relegated to CH extending vibration.

Pyridine ring modes

The ring extending vibrations are critical in the range of pyridine and its subsidiaries and are very normal for the aromatic ring itself. The C-N stretching modes are observed in the range 1300-1000 cm^{-1} [38, 39]. Silverstein [40] assigned C-N stretching absorption in the region 1382-1266 cm-1 for aromatic amines. Silverstein [40] appointed C-N extending

Table 2. The observe FT-IR, FT-Raman and calculated frequencies (in cm^{-1} using B3LYP/6-311+G(d,p) along with their relative intensities, probable assignments reduced mass an force constants of 2-Amino-6-Methyl pyridine.

Observed frequencies (cm^{-1})		Calculated frequencies (cm^{-1})		Force constant (mydn (Å))	IR intensity (km/mol)	Raman activity ($Å^4amu^{-1}$)	Assignments (TED%)
FT-IR	FT-Raman	Unscaled	Scaled				
		3694	3536	8.85	29.01	53.50	??NH_{2as}(99)
3324		3480	3331	7.90	36.15	192.19	??NH_{2ss}(99)
3177		3193	3152	6.58	9.91	179.34	??CH(98)
	3066	3180	3044	6.51	18.86	100.52	??CH(98)
		3164	3051	6.41	5.84	76.20	??CH(97)
		3112	3000	6.29	18.34	61.78	??$CH_{3\ ss}$(98)
		3088	2977	6.18	12.47	84.47	??$CH_{3\ as}$(98)
2922	2922	3033	2922	5.61	20.72	226.07	??$CH_{3\ ips}$(98)
1609		1647	1610	3.06	304.61	20.66	$NH_{2\ sciss}$(69)+??CC(18)
1580		1625	1578	3.64	33.60	2.42	??CC(76)+$NH_{2\ sciss}$(12)
	1469	1619	1466	7.15	86.26	19.53	??CC(58)+$NH_{2\ sciss}$(29)
1462		1502	1459	1.88	77.52	5.52	CH_{3ipb}+??CC(67)+NH_{2sciss}(20)
		1489	1447	3.49	110.27	1.54	??CC(65)+ ??CN(23) CCH_{ipb}(8)
		1477	1426	1.34	7.57	7.92	CH_{3opb}(91)
		1466	1415	2.45	6.88	4.35	??CN(86)
1379	1377	1410	1361	1.51	6.97	14.93	CH_{3ib}(75)
1335	1336	1349	1321	3.21	55.33	15.10	??CN(53)+ ??C-NH_2(10)+??C-CH_3(11)
1279	1280	1315	1269	4.29	12.69	4.92	??CN(40)+??CC(19)+CCH_{ipb}(15)
1238		1262	1218	1.88	12.45	3.23	??CN(40)+ ??C-CH_3(10)+CCH_{ipb}(11)
1162		1184	1155	1.04	8.08	1.11	bCCH(77)
1115		1122	1107	1.06	6.11	6.17	bCCH(56)+NH_{2wagg}(13)
1078		1101	1064	1.21	8.95	1.38	bCCH(52)+ ??CN(11)
1034		1058	1021	1.05	4.09	0.13	CH_{3ipr}(76)
	994	1025	989	1.10	1.59	15.50	NH_{2rock}(39)+CH_{3ipr}(19)
988		998	988	2.66	5.38	15.49	R_{symd}(52)+CH_{3ipr}(14)
929		992	982	0.76	0.03	0.15	CCH_{opb}(59)
		945	936	1.26	3.07	1.23	R_{asymd}(46)+CH_{3ipr}(15)+NH_{2ipr}(10)
785	780	864	864	0.62	1.20	1.10	CCH_{opb}(53)
	736	794	786	0.86	50.35	1.31	$CH_{3\ opr}$(62)
725		745	738	0.56	12.48	1.35	CCH_{opb}(38)+CNC_{opb}(12)
	573	742	735	1.66	2.01	17.19	$bCCC_{ipb}$(35)
		622	579	0.71	9.65	0.86	$bCCN_{opb}$(31)+CCH_{opb}(29)
		575	535	0.99	6.04	9.17	$bCCC_{ipb}$(29)+CNC_{irb}(27)
		548	510	0.87	3.47	5.70	$bCCC_{ipb}$(26)+CNC_{ipb}(24)
464		503	468	0.21	232.58	1.18	$NH_{2\ wagg}$(45)
		448	443	0.31	3.40	0.42	R_{trigd}(58)+bCC(13)
		444	413	0.35	24.90	0.30	tR_{trig}(49)+CH_{wagg}(17)+CC_{wagg}(13)
		376	350	0.09	59.99	0.59	NH_{2twist}(56)+ R_{trigd}(21)
	317	298	278	0.13	3.47	1.54	CH_{3ipr}(18)+NH_{2rock}(17)
	205	218	203	0.11	15.86	0.25	R_{symd}(44)+CH_{3opb}(11)+NH_{2wagg}(18)
		190	198	0.06	0.43	1.83	tR_{trigd}(23)+CH_{3opb}(11)+NH_{2wagg}(18)

as →asymmetric; ss→ symmetric; *ν* →stretching; ipb→in-plane bending; opb→out-of-plane bending; t→tortion; twist→twisting;

wagg→wagging; siss→scissoring; rock→rocking; Rsymd →ring symmetric deformation; Rasymd →ring asymmetric deformation;

Rtrigd →ring trigonal deformation.

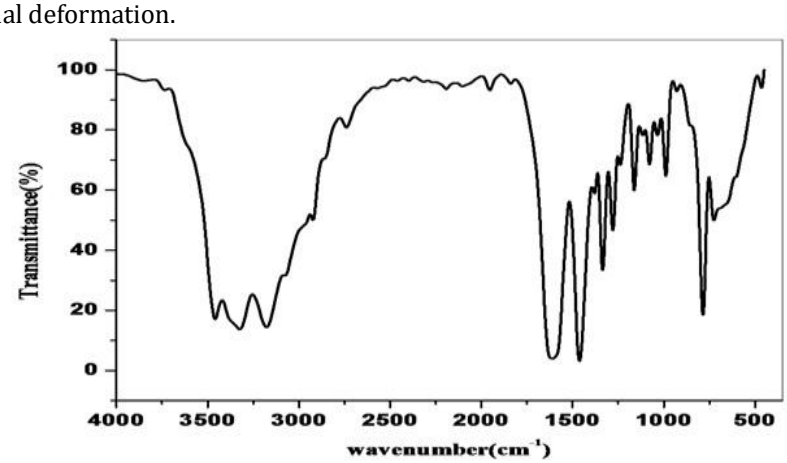

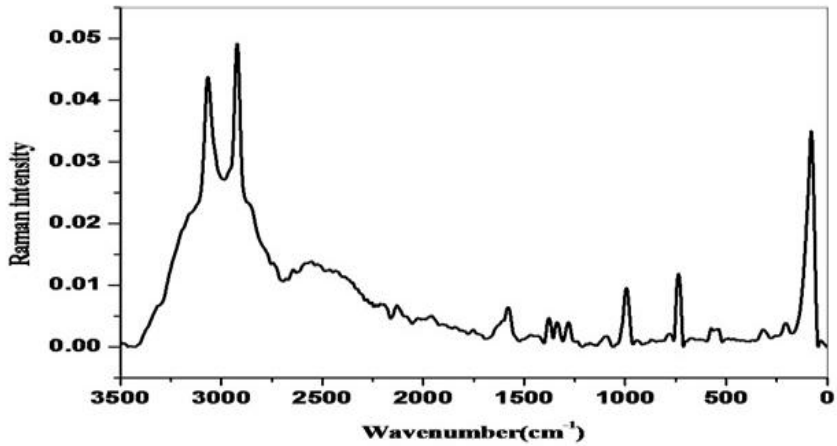

Fig 2. Observed FT-IR and FT-Raman spectra of 2A6MP

absorption in the area 1382-1266 cm^{-1} for aromatic amines. In the present work, C-N stretching modes are assigned at 1280 cm^{-1} in the Raman spectrum, 1279, 1238 cm^{-1} in the IR spectrum and at 1218, 1269 cm^{-1} theoretically with PEDs 40%. The aromatic ring carbon-carbon extending vibrations happen in the area 1430-1625 cm^{-1}[27] and for the title intensify, the C-C aromatic stretch is seen in the area of 1609, 1580 $cm^{-1}$and 1469 cm^{-1} in FT-IR and FT-Raman range, individually. These vibrations are in agreement with the theoretically assignment given by DFT. In general, the C-C vibrations (in-plane and out-of-plane bending) computed by DFT/6-311+G (d, p) methods show good agreement with experimental observation as well as literature value.

Natural Bond Orbital analysis

The NBO examination has been performed on 2A6MP particle in order to clear up intra-molecular charge trade (ICT). The NBO calculations were performed using NBO 3.1[41] program as implemented in the Gaussian 09[22] package and various hyper-conjugative interaction parameters are given in **Tables 3**. The second-arrange bother hypothesis investigation of Fock matrix calculations were done on comparable structure like substitution of H9, H10, H11by Cl9, Cl10, Cl11 substitution (2C2A6MP, 3C2A6MP and 4C2A6MP) in the Pyridine ring modifies the hyper conjugative cooperation's. The important interactions between 'filled' (donor) Lewis type NBO's and 'empty' (acceptor) non-Lewis NBO's of 2A6MP, 2C2A6MP, 3C2A6MP and 4C2A6MP are given in **Table 4**. The second-order perturbation theory analysis of Fock matrix in NBO shows strong intra-molecular hyper conjugative interactions.

The table shows solid intra-molecular hyper conjugative collaborations are framed by orbital cover between LP (N) and BD*(C-C), (C-N) bond orbital which result in intra-molecular charge exchange causing adjustment of the framework. The different critical intra-molecular hyper conjugative associations are: C2-C3 from N1 of LP (N1) BD*(C2-C3) which builds electron density 0.55831e and debilitates the separate securities C2-C3 prompting adjustment of 9.48$KJmol^{-1}$; C2-C3 from N8 of LP (N8) BD*(C2-C3) which expands electron thickness 0.55831e and debilitates the particular securities (C2-C3) prompting adjustment of 5.83$KJmol^{-1}$.

This highest interaction around the ring can induce large bioactivity in the compound. The number of occupancies and energies of most communicating NBOs alongside their level of half and half nuclear orbital's recorded in Table 3. The percentage of hybrid atomic orbital's of nitrogen lone pair atoms, N8 and N1 is partially contributed to both s-type and p-type sub shell, while N8 and N1 is predominantly contributed to P- type sub shell. The P-character of the Nitrogen lone pair orbital's LP (N1) and LP (N8) is 73.69% and 81.51%, respectively. This demonstrates the solitary match orbital takes part in electron gifting in the compound.

The number of intra-molecular hyper conjugative interactions are formed by BD(C-Clx) (x=9, 10, 11) →BD*(C-C) in 4C2A6MP have more energy than other chlorinated substituent's. In 4C2A6MP, the contribution of energy for BD (C5-Cl11→BD*(C5-C6) is 23.27 kcal/mol. For the other chlorinated substituent energy is less for the above interaction. The interaction LP ($Cl_{x=9,10,11}$) →BD*(C-C) was observed only in 2C2A6MP (LP (Cl11) →BD*(C3-C4) shows a large amount of energy (138.66 kcal/mol). These

charge transfer interaction of x2A6MP(x=2C, 3C, 4C) were suggested to highly responsible for pharmaceutical and biological properties.

Table 3.Natural atomic orbital occupancies of most interacting NBO's of 2AMP along with their percentage of hybrid atomic orbitals

ED/energy	BOND(A-B)	ED_B (%)	ED_A (%)	NBO	S(%)	P(%)
1.98272	(C2-C3)	49.32	50.68	$0.7023(sp^{1.58})^+$	38.68	61.28
-0.71451				$0.7119(sp^{1.87})$	34.84	65.11
1.98399	(C2-N1)	40.76	59.24	$0.6385(sp^{2.09})^+$	32.37	67.54
-0.82574				$0.7696(sp^{1.74})$	36.53	63.39
1.72234	(C2-N1)	40.17	59.83	$0.6338(sp^{1.00})^+$	0.00	99.87
-0.29813				$0.7735(sp^{1.00})$	0.01	99.86
1.99053	(C2-N8)	41.08	58.92	$0.6410(sp^{2.48})^+$	28.68	71.22
-0.73358				$0.7676(sp^{2.18})$	31.44	68.48
1.97996	(C3-H9)	60.33	39.67	$0.7767(sp^{2.39})^+$	29.44	70.52
-0.53629				$0.6298(sp^{0.00})$	99.96	0.04
1.98193-0.53861	(C4-H10)	60.36	39.64	$0.7769(sp^{2.43})^+$	29.13	70.83
				$0.6296(sp^{0.00})$	99.96	0.04
1.9774	(C5-H11)	60.38	39.62	$0.7771(sp^{2.48})^+$	28.73	71.23
-0.52769				$0.6294(sp^{0.00})$	99.96	0.04
1.98150	(C6-N1)	40.67	59.33	$0.6377(sp^{2.29})^+$	30.37	69.53
-0.82076				$0.7703(sp^{1.67})$	37.37	62.55
1.90939	LP(N1)			$sp^{2.81}$	26.23	73.69
-0.32030				-		
1.93621	LP(N8)			$sp^{4.42}$	18.43	81.51
-0.31365				-		
0.03757	(C2-C3)	50.68	49.32	$0.7119(sp^{1.58})$	38.68	61.28
0.55831				$-0.7023(sp^{1.87})$	34.84	65.11
0.02943	(C2-N1)	59.24	40.76	$0.7696(sp^{2.09})$	32.37	67.54
0.53478				$-0.6385(sp^{1.74})$	35.53	63.39
0.39734	(C2-N1)	59.83	40.17	$0.7735(sp^{1.00})$	0.00	99.87
0.00571				$-0.6338(sp^{1.00})$	0.01	99.86
0.03452	(C2-N8)	58.92	41.08	$0.7676(sp^{2.48})$	28.68	71.22
0.34196				$-0.6410(sp^{2.18})$	31.44	68.48
0.01436	(C3-H9)	39.67	60.33	$0.6298(sp^{2.39})$	29.44	70.52
0.44218				$-0.7767(sp^{0.00})$	99.96	0.04
0.01276	(C4-H10)	39.64	60.36	$0.6296(sp^{2.43})$	29.13	70.83
0.44532				$-0.7769(sp^{0.00})$	99.96	0.04
0.01569	(C5-H11)	39.62	60.38	$0.6294(sp^{2.48})$	28.73	71.23
0.44594				$-0.7771(sp^{0.00})$	99.96	0.04
0.00436	(C7-H12)	39.03	60.97	$0.6248(sp^{3.11})$	24.35	75.60
0.43155				$-0.7808(sp^{0.00})$	99.97	0.03
0.00381	(C7-H13)	40.09	59.91	$0.6288(sp^{3.15})$	24.10	75.85
0.42154				$-0.7740(sp^{0.00})$	99.97	0.03
0.00724	(C7-H14)	39.54	60.46	$0.6288(sp^{3.16})$	24.02	75.92
0.42178				$-0.7775(sp^{0.00})$	99.97	0.03

Table 4.Comparison of Second-order perturbation theory analysis of Fock matrix in NBO basis corresponding to the intramolecular and bonds of 2A6MP, 2C2A6MP, 3C2A6MP 4C2A6MP.

Donor NBO (i)	Acceptor NBO(j)	$E(2)^a$ (kcal/mol)	$E_{(j)}$-$E_{(i)}{}^b$ (a.u.)	$F_{(i,j)}{}^c$ (a.u.)	$E(2)^a$ (kcal/mol	$E_{(j)}$-$E_{(i)}{}^b$ (a.u.)	$F_{(i,j)}{}^c$ (a.u.)	$E(2)^a$ (kcal/mol)	$E_{(j)}$-$E_{(i)}$ (a.u.)	$F_{(i,j)}{}^c$ (a.u.)	$E(2)^a$ (kcal/mol)	$E_{(j)}$-$E_{(i}$ (a.u.)	$F_{(i,j)}{}^c$ (a.u.)
		2A6MP			2C2A6MP			3C2A6MP			4C2A6MP		
BD(C3 H/C110)	BD*(C2 - C3)	3.32	1.05	0.053	_	_	_	0.84	2.19	0.038	_	_	_
	BD*(C5 - C6)	1.98	1.19	0.044	_	_	_	2.77	0.62	0.04	_	_	_
	BD*(C3 - C4)	_	_	_	_	_	_	14.76	2.12	0.16	_	_	_
	BD*(C4 - C5)	_	_	_	_	_	_	13.91	2.11	0.015	_	_	_
	BD*(C4 -C110)	_	_	_	_	_	_	0.94	2.7	0.045	_	_	_
	BD*(C2 - C3)	_	_	_	_	_	_	2.69	0.58	0.039	_	_	_
	BD*(C4 -C110)	_	_	_	_	_	_	1.64	0.59	0.033	_	_	_

BD(C4 H/C111)	BD*(C3 - C4)	2.73	1.06	0.048	-	-	-	-	-	-	0.64	2.17	0.033
	BD*(C4 - C5)	0.74	1.06	0.025	-	-	-	-	-	-	17.47	2.08	0.173
	BD*(C5 - C6)	2.73	1.2	0.051	-	-	-	-	-	-	23.27	2.22	0.207
	BD*(C5 -C111)	-	-	-	-	-	-	-	-	-	0.99	2.67	0.046
	BD*(C6 – N1)	-	-	-	-	-	-	-	-	-	3.45	2.15	0.077
BD(C2 - H/C19)	BD*(C2 – N1)	4.61	1.03	0.062	1.51	2.15	0.051	-	-	-	-	-	-
	BD*(C3 – C4)	0.54	1.05	0.021	0.84	2.17	0.028	-	-	-	-	-	-
	BD*(C4 – C5)	3.55	1.05	0.055	1.03	2.69	0.042	-	-	-	-	-	-
	BD*(C2 – C3)	-	-	-	14.63	2.09	0.16	-	-	-	-	-	-
	BD*(C4 – C4)	-	-	-	16.05	2.1	0.166	-	-	-	-	-	-
	BD*(C3 -C19)	-	-	-	1.11	2.1	0.049	-	-	-	-	-	-
	BD*(C3 -C19)	-	-	-	1.22	1.13	0.041	-	-	-	-	-	-
	BD*(C4 - H10)	-	-	-	0.75	1.73	0.025	-	-	-	-	-	-
LP(N1)	BD*(C2-C3)	9.48	0.88	0.083	8.79	0.81	0.076	79.66	0.18	0.118	8.35	0.89	0.078
	BD*(C5-C6)	9.46	0.95	0.086	10.51	1.03	0.094	66.71	0.21	0.12	11.4	0.94	0.093
	BD*(C2-N8)	4.4	0.66	0.049	2.61	0.71	0.039	-	-	-	2.62	0.72	0.039
	BD*(C6-C7)	-	-	-	1.87	0.79	0.035	-	-	-	1.85	0.78	0.034
	BD*(C7-H13)	-	-	-	0.86	0.74	0.023	-	-	-	-	-	-
	BD*(C7-H13)	-	-	-	-	-	-	-	-	-	0.89	0.73	0.023
LP(N8)	BD*(C2-C3)	5.83	0.87	0.064	7.71	0.71	0.066	9.34	0.25	0.046	5.01	0.77	0.056
	BD*(C2-N1)	2.57	0.85	0.042	8.48	0.25	0.044	7.21	0.76	0.067	8.7	0.24	0.045
LP(C110)	BD*(C3-C4)	-	-	-	-	-	-	5.19	1.42	0.078	-	-	-
	BD*(C4-C5)	-	-	-	-	-	-	4.85	1.42	0.075	-	-	-
	BD*(C2-C3)	-	-	-	-	-	-	2.41	0.89	0.042	-	-	-
	BD*(C3-C4)	-	-	-	-	-	-	27.04	0.82	0.134	-	-	-
	BD*(C4-C5)	-	-	-	-	-	-	27	0.82	0.134	-	-	-
	BD*(C5-C6)	-	-	-	-	-	-	2.35	1.03	0.045	-	-	-
LP(C19)	BD*(C2-C3)	-	-	-	4.03	141	0.069	-	-	-	-	-	-
	BD*(C3-C4)	-	-	-	4.93	1.41	0.075	-	-	-	-	-	-
	BD*(C2-N1)	-	-	-	2.48	0.86	0.042	-	-	-	-	-	-
	BD*(C3-C4)	-	-	-	28.48	0.81	0.137	-	-	-	-	-	-
	BD*(C4-C5)	-	-	-	2.59	0.88	0.044	-	-	-	-	-	-
	BD*(C2-N1)	-	-	-	0.75	0.35	0.014	-	-	-	-	-	-

[a]E(2) means energy of hyper-conjugative interactions (stabilization energy in lJ/mol).
[b]Energy difference (a.u.) between donor and acceptor i and j NBO orbitals.
[c]F(I,j) is the Fock matrix elements (a.u.) between I and j NBO orbitals.

Frontier molecular orbital analysis

To comprehend the firmness and responsive properties of explored compounds have studied frontier molecular orbitals. To be specific, the most elevated involved molecular orbital (HOMO) and least vacant molecular orbital (LUMO) are the principle molecular orbital's that participate in responses with other molecular structures. Conveyance of HOMO and LUMO gives imperative understanding into the reactive properties of organic molecules [42]. Visual in Fig. 3 demonstrates that HOMO is delocalized over C5-C6 and LUMO is delocalized over N1-C2.

Electro negativity (χ), hardness (η), softness (s), electrophilicity index (ω) and dipole moment are ordinarily utilized as worldwide reactivity parameters inside density functional theory. In the present examination, the HOMO and LUMO energies gap (ΔE), absolute electronegativity, absolute hardness and electrophilicity index of the 2A6MP molecules were registered by B3LYP/6-311+G(d, p). The accounted HOMO and LUMO energies of the title compound was observed to be -6.7672eV and 0.2882eV. As per Koopmans's hypothesis [43] the ionization potential (IP) and electron affinity (EA) can be expressed through HOMO and LUMO orbital energies: Ionization Potential (IP) = $-$EHOMO = 6.7672eV, Electron affinity (EA) ELUMO -0.2882eV [44]. The electro negativity (χ), characterized by Mulliken [45] as the mean of ionization potential (IP) and electron affinity (EA): Electro negativity (χ) $=\frac{IP+EA}{2} = 3.2395$ eV. The hardness of an molecule is identified with the

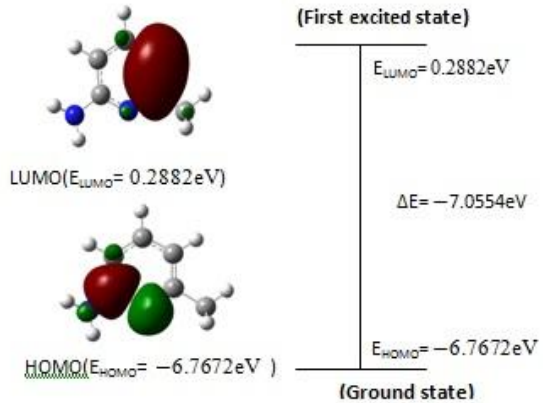

Fig. 3. The HOMO and LUMO diagrams of 2A6MP

gap between the HOMO and LUMO orbital's. The bigger the HOMO-LUMO energy gap, the harder will be the molecule [46].Chemical hardness can be calculated as follows: Chemical hardness $(\eta) = \frac{IP-EA}{2} = 3.5277$ eV. The global softness is the inverse of global hardness: Softness (S) $= \frac{1}{\eta} = 0.2835$eV. The electron affinity in blend with ionization energy likewise give chemical potential (μ) characterized by Parr and Pearson [47] as a property of the electronegative molecules, Chemical potential $(\mu) = -\frac{IP-EA}{2} = -3.5277$ eV. Parr and Yang [48] have presented the worldwide electro philicity record which estimates the tendency of a species to acknowledge electrons. It tends to be computed by utilizing the electronic chemical potential (μ) and chemical hardness (η).Electrophilicity index$(\omega) = \frac{\mu^2}{2\eta} = 0.25$eV. It has been found from the examination of the responsive descriptors that the chemical hardness of the title molecule was observed to be 3.5277eV which is similarly high. While its electro negativity value is nearly high uncovering that the compound is equipped for showing certain organic movement. Additionally, the dipole snapshot of the title compound showed that the compound can get high energy flow out of electrophile to nucleophile .

NLO and HOMO-LUMO analysis

The sizes of hyper polarizabilities are unequivocally upgraded by hydrogen holding. The lion's share of molecular crystals with hydrogen bonding tends to improve the NLO impacts in the crystal structure [53]. So the hydrogen bonds might be utilized as NLO useful bonds in the material designing. The theoretical estimation is by all accounts more accommodating in the assurance of specific segments of β tensor than in building up the genuine estimations of β.

The extensive estimation of polarizability, β, might be expected to π-electron cloud from contributor to acceptor which can make the molecule profoundly polarized and the intermolecular charge exchange (intermolecular hydrogen bonding). The nearness of intra-molecular charge exchange cooperation and the intermolecular hydrogen bonding is affirmed with the vibrational investigation and NBO examination.

The ascertained polarizability and first polarizability of 2A6MP, 3Cl2A6MP, 4Cl2A6MP and 5Cl2A6MP are outlined in Table 5. As can be seen from **Table 5**, the measured first hyper polarizability values have been observed to be 2.5243x10^{-31}esu. for 2A6MP, 4.0155x10^{-31}for 2C2A6MP, 3.4096 x10^{-31}for 3C2A6MP and 1.5989x x10^{-31}for 4C2A6MP at DFT/B3LYP/6-311+G(d, p) technique. The β esteem for 2C2A6MP is bigger incentive than the others. The explanation behind this might be area of NH2 and CH3 cluster.

Table 5. The Predicted polarizability and first hyperpolarizability of 2A6MP, 2C2A6MP, 3C2A6MP and 4C2A6MP

α components	Polarizability(a.u)				β	First hyperpolarizabilities(a.u)			
	2A6MP	2C2A6MP	3C2A6MP	4C2A6MP	components	2A6MP	2C2A6MP	3C2A6MP	4C2A6MP
xx	-39.971			-52.827	xxx	-20.83	19.996	-24.14	21.638
yy	-47.9505			-60.4403	yyy	11.504	-2.589	-15.7	-13.42
zz	-49.3383			-59.2876	zzz	0.0827	0.0525	-0.074	0.0076
xy	2.2314	5.7677	-57.1642	-59.8311	xyy	-2.8749	16.2512	7.0239	-6.9852
xz	-0.7655	1.2584	-57.2652	-53.705	yxx	-6.212	1.0218	-14.1512	-1.3711

yz	1.5677	-1.1461	-59.3044	-59.315	zxx	4.7645	4.4658	-6.5382	1.975
α_{tot}	-45.7533	-57.9113	-57.617	-57.5183	xzz	-5.4565	9.9953	-1.1084	-0.4144
	1.05	1.11	1.02	8.99					
Δα	$X10^{-24}$esu	$X10^{-24}$esu	$X10^{-24}$esu	$X10^{-24}$esu	yzz	-6.8161	6.1291	-5.1381	2.992
					zyy	-3.8032	-5.5709	5.6348	-1.2065
						2.5243	4.0155	3.4096	1.5989
					β_{tot}	$X10^{-31}$esu	$X10^{-31}$esu	$X10^{-31}$esu	$X10^{-31}$esu

examination of the electronics progress demonstrates the change starting from the ground to the first excited state and is basically depicted by one-electron excitation from the most occupied sub-atomic orbital (HOMO) to the least empty orbital (LUMO). This examination uncovers that these molecular systems have vast first static hyper polarizabilities and may have potential applications in the advancement of NLO materials. Atomic HOMOs and LUMOs have been register utilizing Gaussian 09 computer program. The HOMO, LUMO and energy gap estimations of 2A6MP, 2C2A6MP, 3C2A6MP and 3C2A6MP are given in **Table 6.** The energy gap for 2C2A6MP is higher than the others.

Table 6. Comparison of HOMO-LUMO energy gap for the constituents of 2A6MP, 2C2A6MP, 3C2A6MP and 4C2A6MP.

	2A6MP (a.u.)	2C2A6MP (a.u.)	3C2A6MP (a.u.)	4C2A6MP(a.u.)
HOMO	-0.23497	-0.19671	-0.22198	-0.20064
LUMO	-0.04153	-0.04638	-0.04091	-0.04554
HOMO-LUMO Energy gap	-0.19344	-0.15033	-0.18107	-0.1551

As it tends to be seen, the molecular structure of 2A6MP, 2C2A6MP, 3C2A6MP and 4C2A6MP having the higher β_{tot} value, when compared to the low HOMO-LUMO energy gap. This outcome demonstrates HOMO-LUMO energy graphs impacts on the main hyper polarizabilities. The higher β_{tot} value and the comparing low HOMO-LUMO energy gap indicate 2A6MP, 3C2A6MP, 4C2A6MP and 5C2A6MP structures is exceedingly NLO dynamic material [54]. This plainly demonstrates the strong hydrogen bonding between the charged species diminishes the energy gap extensively with the arrangement of the charge exchange hub [55].

Molecular docking

PASS analysis [56]of the title compound predicts activities the top four activitiesTaurine dehydrogenase inhibitor, CDP-glycerol glycerophosphotransferase inhibitor, Membrane integrity agonist, Leukopoiesis stimulantwith probability to be active (Pa) value were 0.857, 0.829, 0.824 and 0.785 respectively(Table 7).High resolution crystal structure of the corresponding inhibitors triclinic ternary complex (6ADH), glycerol-3-phosphate cytidylyltransferase(1COZ), beta1 adrenergic receptor (2Y02) and antimicrobial peptidase lysostaphin(4LXC), were downloaded from the protein data bank website and these receptors are used as target for docking study.PatchDock is a very efficient algorithm for protein–small ligand and protein–protein docking and is a geometry-based molecular docking algorithm [57, 58]. It is aimed at finding docking transformations that yield good molecular shape complementarity. The algorithm was verified on enzyme–inhibitor and antibody–antigen complexes from benchmark 0.0 [59], where it successfully found near-native solutions for most of the cases. The PatchDock algorithm divides the Connolly dot surface representation [60] of the molecules into concave, convex and flat patches. Then, complementary patches are matched in order to generate candidate transformations. Each candidate transformation is further evaluated by a scoring function that considers both geometric fit and atomic desolvationenergy [61]. Finally, an RMSD (root mean square deviation) clustering is applied to the candidate solutions to discard redundant solutions. The main reason behind PatchDock's high efficiency is its fast transformational search, which is driven by local feature matching rather than brute force searching of the six-dimensional transformation space. The ligand title molecule and proteins retrieved from protein data bank are in PDB format submitted to the PatchDock Server.PatchDock Server, aweb page is generated to show the predicted solutions, downloading and viewing the solutions. The detailed ligand-receptor interactions are viewed using Discovery Studio Visualizer 4.0 software.The ligand binds at the active site of the substrate by weak non-covalent interactions. In the case of ligand withtriclinic ternary complexinteractions are detailed in Fig.4a. Aminoacids Glu107 forms H-bond π-alkyl and π-anion interaction with pyridine ring, Gly108 forms H-bond with NH2 group and Val186, Lys185 forms alkyl interaction with methyl group of the title compound. For the amino acids of glycerol-3-phosphate cytidylyltransferaseinteractions with ligand as shown in Fig.4b. Tyr forms H-bond and π- π stacked

interaction with pyridine ring and NH_2 group. Tyr15, His550, His554 shows π-alkyl interaction with methyl group while Glu125 has a H-bond with NH_2 group. In Fig.4c, the residues of beta1 adrenergic receptorPro196 forms H-bond with NH_2 group and Trp182, Cys114 having π-alkyl interaction with pyridine ring and methyl group of the title compound. For antimicrobial peptidase lysostaphin (Fig.4d), the residues Asn372, His362, Met328 forms H-bond, π- π stacked, alkyl interaction with NH_2 group, methyl group respectively while His329, Ile274 shows π-alkyl interaction with pyridine ring. The docked ligand title compound forms a stable complex with the four receptors (Fig.5)with lowest ten minimum conformation of Patch Dock Energyvalues are tabulated in Table.8 These preliminary results suggest that the compound might exhibit inhibitory activity against these receptors.

Table 7.PASS prediction for the activity spectrum of the title compound.

Pa[a]	Pi[b]	Activity
0.857	0.005	Taurine dehydrogenase inhibitor
0.829	0.024	CDP-glycerol glycerophosphotransferase inhibitor
0.824	0.031	Membrane integrity agonist
0.785	0.003	Leukopoiesis stimulant
0.779	0.005	Corticosteroid side-chain-isomerase inhibitor
0.775	0.005	Pterindeaminase inhibitor
0.784	0.014	Glucose oxidase inhibitor
0.79	0.021	Mucomembranous protector
0.741	0.013	Complement factor D inhibitor
0.732	0.006	Amine dehydrogenase inhibitor
0.71	0.013	IgA-specific serine endopeptidase inhibitor
0.71	0.019	Omptin inhibitor
0.714	0.025	NADPH peroxidase inhibitor
0.704	0.026	Glutamylendopeptidase II inhibitor
0.681	0.007	Laccase inhibitor
0.703	0.03	Methylenetetrahydrofolate reductase (NADPH) inhibitor
0.69	0.018	Venombin AB inhibitor
0.68	0.008	Alopecia treatment
0.732	0.062	Phobic disorders treatment

[a]Probability to be active
[b]Probability to be inactive.

Table 8. The top ten conformation of the complex candidate of ligands
Table 8.1 with triclinic ternary complex

No.	glob	aVdw	rVdw	ACE
1	-21.39	-9.47	0.42	-4.74
2	-21.05	-7.82	0.16	-6.15
3	-20.14	-8.11	0.4	-5.22
4	-20.02	-9.05	1.08	-4.82
5	-19.32	-8.81	0	-4.04
6	-17.89	-8.97	0.08	-3.61
7	-17.76	-6.45	1.56	-5.97
8	-17.41	-9.17	0	-2.64
9	-15.79	-5.45	0	-5.04
10	-14.32	-7.94	1.82	-3.16

Table 8.2 with glycerol-3-phosphate cytidylyltransferase				
1	-16.87	-7.88	1.21	-4.78
2	-16.61	-7.33	0.83	-4.22
3	-16.05	-9.27	2.92	-3.03
4	-15.75	-6.89	0.44	-3.97
5	-14.21	-8.56	3.36	-3.28
6	-11.79	-7.48	0.53	-1.89
7	-11.45	-7.32	0.5	-1.49
8	-9.39	-6.18	0.05	-2.01
9	-6.84	-3.55	0.77	-2.9
10	-2.76	-4.37	1.1	-0.31
Table 8.3 with beta1 adrenergic receptor				
1	-26.46	-8.91	0.36	-8.49
2	-21.41	-8.04	0.22	-6.7
3	-20.68	-9.21	1.4	-5.6
4	-19.86	-7.75	0.24	-5.4
5	-19.69	-7.76	0.47	-5.48
6	-19.34	-7.74	0.51	-5.65
7	-18.69	-8.08	1.26	-5.15
8	-18.26	-9	2.17	-4.19
9	-15.97	-7.3	0	-3.74
10	-14.58	-7.28	0.79	-4.33
Table 2.4 with antimicrobial peptidase lysostaphin				
1	-23.16	-11.93	3.05	-4.93
2	-18.91	-9.21	0.6	-3.52
3	-18.65	-7.97	0.21	-4.48
4	-17.44	-8.05	0.05	-3.39
5	-16.65	-6.29	0.1	-4.61
6	-15.72	-7.05	0.07	-3.36
7	-14.45	-7.1	0.13	-3.02
8	-13.33	-7.92	0	-1.75
9	-12.57	-8.08	1.71	-1.57
10	-10.58	-6.63	0.24	-0.67

glob - Global Energy (kcal/mol) (binding energy of the solution);
aVdW and rVdW - softened attractive and repulsive van der Waals energy;
ACE - atomic contact energy (ACE)

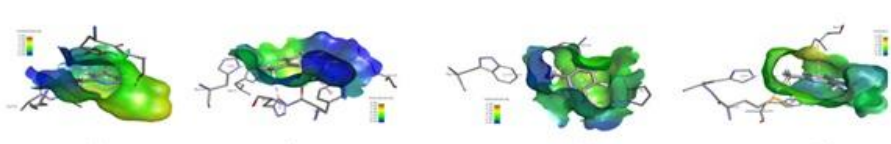

Fig. 4.The interactive plot of docked ligand with residues of (a) triclinic ternary complex and hydrophobic surface shown (b) glycerol-3-phosphate cytidylyltransferase and hydrophobic surface shown (c) beta1 adrenergic receptorand hydrophobic surface shown (d) antimicrobial peptidase lysostaphinand hydrophobic surface shown

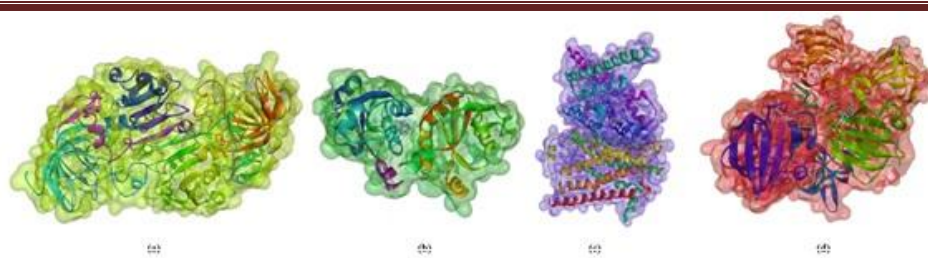

Fig. 5. The docked ligand at the active sites of (a) triclinic ternary complex (b) glycerol-3-phosphate cytidylyltransferase (c) beta1 adrenergic receptor (d) antimicrobial peptidase lysostaphin

Conclusion

The improved geometric parameters of title compound were deciphered and equated with the before announced experimental values for a comparable compound. The FT-IR and FT-Raman spectra of 2A6MP were recorded and vibrational modes were allotted with the guide of the trial and figured vibrational wave numbers and their TEDs. The second-order perturbation theory investigation of fock network, ESP, energy gap, polarizability and first hyper polarizability counts were performed on x2A6MP(x=2C, 3C, 4C). As indicated by the computed outcomes of ESP, the normal greatest negative electrostatic potential estimation of x2A6MP(x=2C, 3C, 4C), increment all together in the order of2A6MP→3C2A6MP →4C2A6MP →

2C2A6MP. Low estimation of HOMO LUMO energy gap proposes the likelihood of intra-molecular charge move in the molecule. This assumes a vital part in the huge increment of β value, which is an addictive property to show non-linear optical movement. The NBO investigation uncovers hyper conjugative cooperation, ICT and adjustment of molecule. The examination of NBO estimations of x2A6MP(x=2C, 3C, 4C) proposes the pharmaceutical properties of 2C2A6MP was more noteworthy than the others. The molecular docking experiments demonstrates that the docked ligand, title compound compound steady complex with pyridine inhibitor and gives a binding affinity value of - 4.75 Kcal/mol and this outcome recommends that the compound may show inhibitory action against cyclin-subordinate kinase 2 (CDK2). It is believed that the results of the current theoretical investigations could support the development of clinical applications.

Reference

1. S.P. Jose, S. Mohan, Vibrational spectra and normal co-ordinate analysis of 2-aminopyridine and 2-amino picoline. Spectrochim Acta A Mol Biomol Spectrosc 64 (2006) 240–245.
2. K. Othmer,Encyclopedia of chemical technology, 4th edn, vol. 20. Wiley, New York, 1997.
3. P. Pierrat , P.C. Gros ,Y. Fort, Solid phase synthesis of pyridine-based derivatives from a 2-chloro-5-bromopyridine scaffold., J. Comb. Chem. 7 (2005) 879–886.
4. C. Jr Temple , J.D. Rose, R.N. Comber , G.A Rener, Synthesis of potential anticancer agents: imidazo[4,5-c]pyridines and imidazo[4,5-b]pyridines., J. Med. Chem. 30(10) (1987) 1746–1751.
5. F. Janssens , J. Torremans , M. Janssen , R.A. Stokbroekx , M. Luyckx , P.A.J. Janssen, New antihistaminic N-heterocyclic 4-piperidinamines. 3. Synthesis and antihistaminic activity of N-(4-piperidinyl)-3H-imidazo[4,5-b]pyridin-2-amines., J. Med. Chem., 28 (1985) 1943–1947.
6. "Iodine Solution (0.02 M in THF/pyridine/H2O 70:20:10)". Sigma-Aldrich. Retrieved 28 November 2011.
7. https://en.wikipedia.org/wiki/Pyridine
8. D.R. Lide , ed., Handbook of Chemistry and Physics (90th ed.). BocaRaton: CRC Press. ISBN 978-1-4200-9084-0, 2009.
9. "Pyridine hydrochloride MSDS" (PDF). Alfa Aesar. Retrieved 26 June 2010.
10. J. A. Joule, K. Mills,Heterocyclic Chemistry (5th ed.). Chichester: Blackwell Publishing. SBN 1-4051-3300-7, 2010.
11. D.T. Davies, Aromatic Heterocyclic Chemistry. Oxford University Press. ISBN 0-19-855660-8, 1992.
12. R. Milcent , F. Cha, Chimie organique hétérocyclique: Structures fondamentales. EDP Sciences. pp. 241–282.ISBN 2-86883-583-X, 2002.
13. "IUPAC SC-Database: A comprehensive database of published data on equilibriumconstants of metal complexes and ligands".
14. R. Kubiak , J. Janczak , M. Sledz,Crystal structures of 2- and 3-cyanopyridine., J. Mol. Struct., 610 (2002) 59–64.
15. R.G. Ford,The microwave spectra and dipole moments of the cyanopyridines., J. Mol. Spectrosc., 58 (1975) 178–184.
16. J.F. Arenas, I.L. Tocón, J.C. Otero, J.I. Marcos, Vibrational spectrum of 2-methylpyridine., J. Mol. Struct., 410 (1997) 443–446.

17. N. Sundaraganesan , S. Ilakiamani , H. Saleem , P.M. Wojciechowski, Michalska , DFT-Raman and FT-IR spectra, vibrational assignments and density functional studies of 5-bromo-2-nitropyridine., Spectrochim. Acta. A Mol. Biomol. Spectrosc. 61(2005a) 2995–3001.
18. S.F. Tayyari , S.J. Mahdizadeh , S. Holakoei , Y.A. Wang, Vibrational assignment and proton tunneling in pyridine–pyridinium complexes., J. Mol. Struct. 971(2010) 39–46, 2010.
19. C.S. Hiremath , J. Yenagi , J. Tonannavar , T. Sundius , Ab initio/DFT electronicstructure calculations, spectroscopic studies and normal coordinate analysis of 2-chloro-5-bromopyridine. Spectrochim. Acta. A Mol. Biomol. Spectrosc.77(2010) 918–926.
20. A. Davoodnia , P. Attar ,A. Morsali ,H. Eshghi , N.T. Hoseini , S. Khadem, Experimental and theoretical studies on the tautomerism in 2-aminopyridines and 2(1H)-pyridinones: synthesis of 2-amino-4-aryl-3-cyano-6-(3,4-dimethoxyphenyl)pyridines and 4-Aryl-3-cyano-6-(3,4-dimethoxyphenyl)-2(1H)-pyridinones., Bull Korean Chem. Soc, 32(6) (2010) 1873–1878.
21. E. Spinner,Vibration spectra and structures of the hydrochlorides of aminopyridines, J. Chem. Soc., 0 (1962) 3119–3126.
22. M. J. Frisch, G. W. Trucks, H. B. Schlegel, G. E. Scuseria, M. A. Robb, J. R. Cheeseman, G. Scalmani, V. Barone, B. Mennucci, G. A. Petersson, H. Nakatsuji, M. Caricato, X. Li, H. P. Hratchian, A. F. Izmaylov, J. Bloino, G. Zheng, J. L. Sonnenberg, M. Hada, M. Ehara, K. Toyota, R. Fukuda, J. Hasegawa, M. Ishida, T. Nakajima, Y. Honda, O. Kitao, H. Nakai, T. Vreven, J. A. Montgomery, Jr., J. E. Peralta, F. Ogliaro, M. Bearpark, J. J. Heyd, E. Brothers, K. N. Kudin, V. N. Staroverov, R. Kobayashi, J. Normand, K. Raghavachari, A. Rendell, J. C. Burant, S. S. Iyengar, J. Tomasi, M. Cossi, N. Rega, J. M. Millam, M. Klene, J. E. Knox, J. B. Cross, V. Bakken, C. Adamo, J. Jaramillo, R. Gomperts, R. E. Stratmann, O. Yazyev, A. J. Austin, R. Cammi, C. Pomelli, J. W. Ochterski, R. L. Martin, K. Morokuma, V. G. Zakrzewski, G. A. Voth, P. Salvador, J. J. Dannenberg, S. Dapprich, A. D. Daniels, O. Farkas, J. B. Foresman, J. V. Ortiz, J. Cioslowski, and D. J. Fox, Gaussian, Inc., Wallingford CT, 2009.
23. H.B. Schlegel, Optimization of equilibrium geometries and transition structures, J. Comput. Chem., 3(1982) 214.
24. S. Ramalingam, S. Periandy, S. Mohan, Vibrational spectroscopy (FTIR and FTRaman) investigation using ab initio (HF)and DFT (B3LYP and B3PW91) analysis on the structure of 2-amino pyridine, Spectrochim. Acta 77A (2010) 73–81.
25. Madhukar Hemamalini, Ibrahim Abdul Razak and Hoong-Kun Fun,2-Amino-6-methylpyridinium 2-carboxybenzoate, Acta Cryst., E67 (2011) o2402.
26. K. Syed Suresh Babu, M. Dhavamurthy, M. NizamMohideen, G. Peramaiyan, R. Mohan, 2-amino-6-methylpyridinium 4-methyl-benzenesulfonate, Act. Cryst., E70 (2014) o600-o601.
27. S.M. Bakalova, A.G. Santos,L. Timchev, J.Kaneti,I.L. Filipova, G.M. Dobrikov, V.D. Dimitrov,A Computational Study of the Diels– Alder Reaction of Ethyl-S-lactyl Acrylate and Cyclopentadiene, J. Mol. Struct. Theochem., 710 (2004) 229–234.
28. D.N. Sathyanarayana, Vibrational Spectroscopy, New Age International Publishers, 2007.
29. G. Socrates, Infrared, Raman Characteristic Group Frequencies, Tables and Charts, third ed., Willey, Chichester, 2001.
30. H. Kaur, Spectroscopy, second edition, Pragati Prakashan, Meerut, 2004-2005.
31. D. Lin Vien, N.B. Colthup, W.G. Fateley, J.G. Grasselli, the Handbook of Infrared and Raman characteristic Frequencies of organic molecules, Acaemic Press, 1991.
32. S.F. Parker, Vibrational spectroscopy of N-methylmaleimide, Spectrochimica Acta., A51(1995) 2067−2072.
33. A.B. Dempster, D.B. Powell, N. Sheppard, Vibrational spectroscopic studies of internal rotation of symmetrical groups—III: Toluene and some deuterated derivatives in the condensed state, spectrochimica Acta., 28A (1972) 373−379.
34. W.O. George, S. Mcintyre, Introduction to spectroscopy, John Willey, New York.
35. N.P. Roeges, A Guide to the complete interpretation of Infrared spectra of organic structures, Willey, New York, 1994.
36. G.Varsanyi, Vibrational Spectra of 700 Benzene Derivatives, vol.I-II, Academic Kiaclo,
    a. Budapest. 1973.
37. B. Smith, Infrared Spectral Interpretation, A. Systematic Approach, CRC press, Washington, DC, 1999.
38. L.H.D.N.B. Colthup, S.E. Wiberly, Introduction to IR and Raman Spectroscopy, Academic Press,. TS-CrossRef Metadata Search M4-Citavi, New York, 1990.
39. R.M. (Robert M. Silverstein), F.X.Webster, D.J.Kiemle, and D.L(David L Bryce), Spectrometric Identification of Organic Compounds .
40. M. Silverstein, G. Clayton Basseler, C. Morill, Spectrometric Identification of Organic Compounds, Wiley, Newyork, 1981.
41. E.D. Glendening, A.E. Reed, J.E. Carpenter, F. Weinhold, NBO Version 3.1, Gaussian Inc., Pittsburgh, PA, 2003.
42. G. Gece, The use of quantum chemical methods in corrosion sciences, Corros.Sci. 50, (2008) 2981-2922.

43. T. Koopmans, Über die Zuordnung von Wellenfunktionen und Eigenwerten zuden einzelnen Elektronen eines Atoms, Physica 1 (1-6) (1934) 104-113.
44. S.H.R. Sebastian, M.A. Al-Alshaikh, A.A. El-Emam, C.Y. Panicker, J. Zitko, M. Dolezal, C. Van Alsenoy, Spectroscopic, quantum chemical studies, Fukui functions, in vitro antiviral activity and molecular docking of 5-chloro-N-(3-nitrophenyl)pyrazine-2-carboxamide, J. Mol. Struct. 1119 (2016) 188-199.
45. R.S. Mulliken, A new electroaffinity scale; together with data on valence states and on valence ionization potentials and electron affinities, J. Chem. Phys. 2 (11) (1934) 782-793.
46. R.G. Pearson, Absolute electronegativity and hardness correlated with molecular orbital theory, Proc. Natl. Acad. Sci., 83 (22) (1986) 8440-8441.
47. R.G. Parr, R.G. Pearson, Absolute hardness: companion parameter to absolute electronegativity, J. Am. Chem. Soc. 105 (26) (1983) 7512-7516.
48. R.G. Parr, W. Yang, Density-functional theory of the electronic structure of molecules, Annu. Rev. Phys. Chem. 46 (1) (1995) 701-728.
49. E. Temel, C. Alas¸ alvar, H. G€okçe, A.Güder, Ç. Albayrak, Y.B. Alpaslan,G. Alpaslan, N. Dilek, DFT calculations, spectroscopy and antioxidant activity studies on (E)-2-nitro-4-[(phenylimino) methyl] phenol, Spectrochim. Acta A Mol. Biomol. Spectrosc. 136 (2015) 534-546.
50. E. Scrocco, J. Tomasi, Electronic molecular structure, reactivity and intermolecular forces, an euristic interpretation by means of electrostatic molecular potentials, Adv. Quantum Chem. 11 (1978) 115-193.
51. F.J. Luque, J.M. Lopez, M. Orosco, Perspective on electrostatic interactions of a solute with a continuum, a direct utilization of ab initio molecular potentials for the prevision of solvent effects, Theor. Chem. Acc. 103 (2000) 343-345.
52. N. Okulik, A.H. Jubert, Theoretical analysis of the reactive sites of non-steroidal anti-inflammatory drugs, Internet Electron, J. Mol. Des. 4 (2005) 17-30.
53. M. Amalanathan, I. Hubert Joe, Irena Kostova, Density functional theory calculation and vibrational spectral analysis of 4-hydroxy-3- (3-oxo-1-phenylbutyl) -2H-1-benzopyran-2-one, J. Raman Spectrosc. 41 (2009) 1076—1084.
54. M. Amalanathan, I. Hubert Joe, V.K. Rastogi, Density functional theory studies on molecular structure and vibrational spectra of NLO crystal L-phenylalanine phenylalanium nitrate for THz application J.Mole. structe. 1006(2011) 513-526.
55. Ch. Bosshard, R. Spreiter, L. Degiorgi, P. Gunter, Infrared and Raman spectroscopy of the organic crystal DAST: Polarization dependence and contribution of molecular vibrations to the linear electro-optic effect, Phys. Rev. B66 (2002) 205107.
56. A.Lagunin, A.Stepanchikova, D.Filimonov, V.Poroikov, PASS: prediction of activity spectra for biologically active substances, Bioinformatics 16 (2000) 747-748.
57. D.Duhovny, R.Nussinov, H.J.Wolfson, Efficient Unbound Docking of Rigid Molecules, In Gusfield et al., Ed. Proceedings of the 2'nd Workshop on Algorithms in Bioinformatics(WABI) Rome, Italy, Lecture Notes in Computer Science 2452, pp. 185-200, Springer Verlag, 2002.
58. C.Zhang, G.Vasmatzis, J.L.Cornette, C.DeLisi, Determination of atomic desolvation energies from the structures of crystallized proteins, J. Mol. Biol. 267(3) (1997) 707-26.
59. R.Chen, J.Mintseris, J. Janin, Z.Weng, A protein–protein docking benchmark, Proteins, 52 (2003) 88–91.
60. M.L. Connolly, Analytical molecular surface calculation. J. Appl. Cryst. 16 (1983) 548–558.
61. C.Zhang, G. Vasmatzis, J.L.Cornette, C.DeLisi, Determination of atomic desolvation energies from the structures of crystallized proteins. J. Mol. Biol., 267 (1997) 707-726.